Article

Unraveling Electronic and Vibrational Coherences Following a Charge Transfer Process in a Photosystem II Reaction Center

Junhua Zhou [1,†], Xuanchao Zhang [1,†], Vandana Tiwari [2], Chao Mei [1], Ajay Jha [3,4], Pan-Pan Zhang [1] and Hong-Guang Duan [1,*]

1   Department of Physics and Institute of Modern Physics, Ningbo University, Ningbo 315211, China; 2111077059@nbu.edu.cn (J.Z.); 2301690143@nbu.edu.cn (X.Z.); meichao@nbu.edu.cn (C.M.); zhangpanpan@nbu.edu.cn (P.-P.Z.)
2   SLAC National Accelerator Laboratory, Menlo Park, CA 94025, USA; vandanat@stanford.edu
3   Rosalind Franklin Institute, Harwell Campus, Didcot OX11 0QX, UK; ajay.jha@rfi.ac.uk
4   Department of Pharmacology, University of Oxford, Oxford OX1 3QT, UK
*   Correspondence: duanhongguang@nbu.edu.cn
†   These authors contributed equally to this work.

Abstract: A reaction center is a unique biological system that performs the initial charge separation within a Photosystem II (PSII) multiunit enzyme, which eventually drives the catalytic water-splitting in plants and algae. The possible role of quantum coherences coinciding with the energy and charge transfer processes in PSII reaction center is one of the active areas of research. Here, we study these quantum coherences by using a numerically exact method on an excitonic dimer model, including linear vibronic coupling and employing optimal parameters from experimental two-dimensional coherent spectroscopic measurements. This enables us to precisely capture the excitonic interaction between pigments and the dissipation of the energy from electronic and charge-transfer (CT) states to the protein environment. We employ the time nonlocal (TNL) quantum master equation to calculate the population dynamics, which yields numerically reliable results. The calculated results show that, due to the strong dissipation, the lifetime of electronic coherence is too short to have direct participation in the charge transfer processes. However, there are long-lived vibrational coherences present in the system at frequencies close to the excitonic energy gap. These are strongly coupled with the electronic coherences, which makes the detection of the electronic coherences with conventional techniques very challenging. Additionally, we unravel the strong excitonic interaction of radical pair (P_{D1} and P_{D2}) in the reaction center, which results in a long-lived electronic coherence of >100 fs, even at room temperature. Our work provide important physical insight to the charge separation process in PSII reaction center, which may be helpful for better understanding of photophysical processes in other natural and artificial light-harvesting systems.

Keywords: Photosystem II (PSII); quantum coherences; long-lived vibrational coherences; time nonlocal (TNL) quantum master equation

1. Introduction

Photosynthesis is one of the most important light-driven biological processes, which converts light energy into chemical energy through a series of photochemical events. Photon energy absorbed by the light-harvesting antennas is funneled to the PSII reaction center (RC). The PSII RC plays a vital role of utilizing the absorbed photons for efficient separation of electronic charges, which eventually leads to water dissociation and oxygen generation. PSII RC is a multi subunit protein complex, which is embedded in the photosynthetic system and it is structure has been well resolved by X-ray crystallography [1–3]. It contains eight cofactors, symmetrically located along the protein central axis. It contains two primary chlorophylls, P_{D1} and P_{D2}; two accessory chlorophylls, Chl_{D1} and Chl_{D2}; two pheophytins, $Pheo_{D1}$ and $Pheo_{D2}$; and two peripheral chlorophylls, $Chlz_{D1}$ and $Chlz_{D2}$, respectively.

Recent studies have implied that only the D_1 branch is active in the charge separation process in the reaction center, while the D_2 branch shows the capacity for the flowing of extra energy generated by strong light excitation [4]. A detailed protein structure and the pigment locations are shown here in Figure 1.
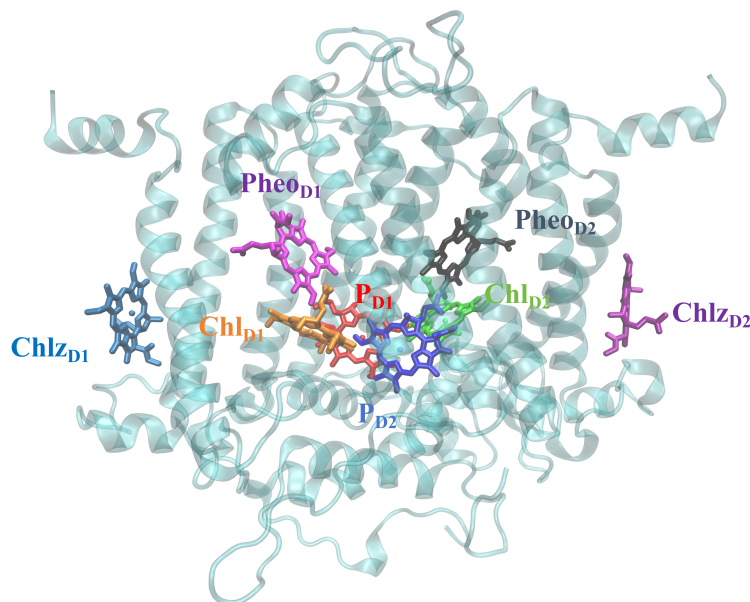

Figure 1. The protein and pigment structure of Photosystem II reaction center (PSII RC). The organization of pigments in the PSII RC is distinctly structured: it includes the central pair of pigments, P_{D1} (red) and P_{D2} (blue), followed by accessory chlorophylls, Chl_{D1} (orange) and Chl_{D2} (green), and pheophytin pigments, $Pheo_{D1}$ (pink) and $Pheo_{D2}$ (gray).

In view of its importance in the efficient conversion of light energy into charges, an enormous amount of experimental and theoretical research work have has performed to study the underlying dynamics of energy and charge transfer processes in the PSII reaction center [5–7]. The photo-echo and transient absorption spectroscopes were performed to measure the dynamics of the primary charge transfer processes in the PSII reaction center [8]. The results show that the primary charge transfer occurs on the timescale of 1.5 ps, while the secondary charge transfer process occurs within 25 ps. To observe a relatively slow reaction process of the secondary charge transfer, Grondelle et al. employed the transient absorption spectroscopy to measure the energy and charge transfer pathways with the extended detection window of 3 ns [9]. The measured data were examined by global and target analyses, and it showed four charge-transfer states participating in two charge transfer processes within the timescales ranging from hundreds of femtoseconds to nanoseconds. Two-dimensional electronic spectroscopy shows the capability of resolving energy, charge transfers and the associated coherent dynamics in pigment protein complexes [10–15]. In 2010, Ogilive et al. employed 2D electronic spectroscopy to study the energy and primary charge transfer dynamics in PSII reaction center [16]. The subsequent data analysis showed the lifetime of energy and charge transfers. Capitalizing on the better sensitivity, they used the 2D electronic spectroscopy to investigate the role of coherence during the energy and charge-transfer processes. The resulting data reported that a long-lived vibrational or vibronic coherences were observed, and it enhanced the efficiency of charge transfer [17]. Moreover, Grondelle et al. measured the 2D electronic spectra of PSII reaction center, and the observed oscillatory dynamics have been assigned to the vibronic quantum coherence during the energy and charge transfer processes. They claimed that this observed vibronic coherence could prolong the lifetime of electronic coherence and enhances the efficiency of charge transfer [18]. However, due to the spectral congestion, the site energies of PSII reaction center have been inconsistent for different

research groups [17,18]. Novoderezhkin et al. developed an exciton model and refined the parameters by a simultaneous fit to the absorption, emission, linear dichroism and circular dichroism spectra [19]. The model and the features of the CT states have been further improved by fitting the model to additional steady-state fluorescence and Stark spectroscopy data [20]. They showed that the refined site energies can be strongly affected during the evolution of refined algorithm and parameters, which shows the difficulties of obtaining the reliable site energies close to the reality. A recent study employed the modified Redfield equation and calculated the time evolved 2D electronic spectra. However, the calculated results still show the obvious difference from experimental observations, which further highlights the difficulty of modeling PSII reaction center with congested absorption features [21]. Although the PSII reaction center has been extensively investigated using these various spectroscopic methods, but the understanding of any functional role of the underlying electronic and vibrational coherences are still not conclusive. Also, the realistic site energies and the dissipative parameters between system and environment are yet to be learn.

Temperature plays one of the most important roles in affecting the system–bath interaction by regulating the rms amplitude and modifying the frequency distribution of the very movements, resulting in collisional randomization of phase or decoherence. Thus, a precise measurement of electronic and vibrational coherences can be performed at lower temperatures. In this paper, we aim to study the PSII RC for the role of electronic and vibrational coherences during the processes of energy and charge transfers. To study these dynamical processes, the model and parameters are taken from our previous results in Ref. [22]. The model could capture the precise dissipation of protein environment by directly comparing the anti-diagonal profile of 2D electronic spectrum at initial waiting time. By this, we could capture the reasonable timescale of electronic and vibrational coherences. For this, we firstly construct a dimer model with two selected pigments, P_{D1} and P_{D2}, Chl_{D1} and $Pheo_{D1}$. Moreover, we select two typical vibrational modes, 340 and 730 cm^{-1}, which have been reported in Refs. [17,18,23]. Moreover, a charge transfer and charge separation states are also included, which allows us to examine any functional role of coherences. We employed the time nonlocal (TNL) quantum master equation to calculate the population dynamics and the associated coherences. The subsequent data analysis of residuals has been performed after removing kinetics by global fitting approach [24]. By this, we are able to capture the reliable site energies and excitonic couplings along with the strength of the system–bath interaction. Our model and refined parameters reveals the detailed dynamics of primary charge transfer and charge separation with the underlying roles of electronic and vibrational coherences.

2. Modeling and Parameters

We firstly start from the dimer model with two additional states, charge transfer and charge separation states. Thus, we have the electronic Hamiltonian, which shows the form

$$H_{ele} = \sum_{i,j} (\epsilon_i i \; \langle i| + V_{ij} |i\rangle \langle j|),$$

(1)

where the ϵ_i is the site energy of site i and V_{ij} is the excitonic coupling between site *i* and *j*. Here, we assume that ϵ_1, ϵ_2 are the Franck exciton states, ϵ_3, ϵ_4 are the charge transfer and charge separation states, respectively. To consider the role of vibrational coherence, we select two common modes with frequencies of 340 and 730 cm^{-1}, which were resolved from 2D spectroscopic measurements [17,18]. We include the vibrational Hamiltonian in the system part, which yields

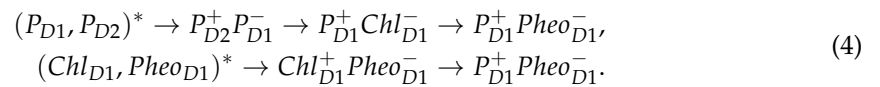$$H_S = \sum_{i,j} (|i\rangle h_i \langle i| + |i\rangle V_{ij} \langle j|),$$

(2)

where $h_i = \epsilon_i + h_g + \kappa_\beta Q_\beta$, $h_g = \frac{1}{2}\sum_{\beta=1,2}\Omega_\beta(P_\beta^2 + Q_\beta^2)$. P_β and Q_β are the momentum and coordinate of each mode, Ω_β is the frequency of the mode. κ_β is the strength of vibrational coupling. Here, we have $\kappa_\beta = \Delta_\beta\Omega_\beta/\sqrt{2}$, where Δ_β is the dimensionless shift of β-th mode. Moreover, to consider the dissipation, we assume the system Hamiltonian linearly couple to a reservoir of harmonic oscillators, which yields $H_{tot} = H_S + H_{env}$. Thus, we have the system–bath interaction and bath Hamiltonian

$$H_{env} = \sum_i\sum_\alpha\left[\frac{p_{i,\alpha}^2}{2m_{i,\alpha}} + \frac{m_{i,\alpha}\omega_{i,\alpha}^2}{2}\left(x_{i,\alpha} + \frac{c_{i,\alpha}\,|i\rangle\,\langle i|}{m_{i,\alpha}\omega_{i,\alpha}^2}\right)^2\right]. \tag{3}$$

Here, the momenta of the bath oscillators is denoted as $p_{i,\alpha}$, while their coordinates, masses and frequencies are denoted by $x_{i,\alpha}, m_{i,\alpha}, \omega_{i,\alpha}$, respectively. The respective coupling constants are $c_{i,\alpha}$. The bath are characterized by the spectral densities $J_i(\omega) = \frac{1}{2}\sum_\alpha\frac{c_{i,\alpha}^2}{m_{i,\alpha}\omega_{i,\alpha}}\delta(\omega - \omega_{i,\alpha})$. In this work, we assume that both modes experience fluctuations with an Ohmic spectral density $J_i(\omega) = \eta_i\omega\exp(-\omega/\omega_c)$. The η_i are the damping strengths for the tuning and coupling modes, respectively. In addition, ω_c is the cutoff frequency, which is assumed, for simplicity, as equal for the two baths. The reorganization energies are given by $R_i = 2\eta_i\hbar\omega_c/\pi$.

3. Results

Using the above described model and parameters, we study the population transfer and associated coherent dynamics of two charge transfer pathways, which is given as

$$\begin{aligned}(P_{D1}, P_{D2})^* &\to P_{D2}^+P_{D1}^- \to P_{D1}^+Chl_{D1}^- \to P_{D1}^+Pheo_{D1}^-,\\(Chl_{D1}, Pheo_{D1})^* &\to Chl_{D1}^+Pheo_{D1}^- \to P_{D1}^+Pheo_{D1}^-.\end{aligned} \tag{4}$$

Firstly, we study the charge transfer of radical pair, P_{D1} and P_{D2}. For this, we directly take the site energies from Ref. [22], which shows $\epsilon_1 = 280$ cm^{-1} and $\epsilon_2 = 210$ cm^{-1}, respectively. The excitonic interaction $V_{12} = 150$ cm^{-1}. Moreover, we also select the charge transfer state $P_{D2}^+P_{D1}^-$ and charge separation state $P_{D1}^+Chl_{D1}^-$. Thus, we have the site energies $\epsilon_3 = 200$ cm^{-1} and $\epsilon_4 = 800$ cm^{-1}, which have been taken from Ref. [21]. The excitonic interactions between excitonic states, charge transfer, and charge separation states are presented in the Supporting Information (SI). In addition, we assume $\eta_1 = \eta_2 = 1.0$ and $\omega_c = 200$ cm^{-1} for the spectral densities of excitonic states. Due to the strong permanent dipole, the charge transfer (separation) state shows stronger system–bath interaction, which yields $\eta_3 = 1.5$ ($\eta_4 = 2.0$). We set the cutoff frequency $\omega_c = 200$ cm^{-1}.

We repeat the same procedure to select the site energies of excitonic, charge transfer and charge separation states for the second pathway in Equation (4). We choose the excitonic states Chl_{D1} and $Pheo_{D1}$, charge transfer $Chl_{D1}^+Pheo_{D1}^-$ and charge separation state $P_{D1}^+Pheo_{D1}^-$. The site energies and excitonic couplings are listed in the next subsection and in the first part of the Supporting Information. With these parameters, we assume the population is equally distributed on excitonic states at initial time and we calculate the population dynamics.

3.1. Energy and Charge Transfers between P_{D1} and P_{D2}

We firstly present the population dynamics and charge transfer of radical pair (P_{D1} and P_{D2}) in Figure 2. The schematic diagram of energy and charge transfer of radical pair are presented in Figure 2a. We set the temperature T = 77 K, and the resulting population dynamics are shown in Figure 2b. The population transfers of excitonic states are plotted as red and blue solid lines, respectively. The charge transfer and charge separation states are plotted as green and magenta solid lines. We observe that, due to the strong excitonic coupling, V = 150 cm^{-1}, the oscillatory dynamics could persist for more than 600 fs in the excitonic states P_{D1} and P_{D2}. Although the system–bath interaction is strong, it still shows a weak oscillatory dynamics in charge transfer and charge separation states. To further

examine the origin of these oscillations, we perform the global fitting procedure and fit the kinetics. The detailed fitting quality and results are shown in the second part of the Supporting Information. After removing the kinetics, we plot the residuals of excitonic and charge transfer states as solid lines in Figure 2c. The associated Fourier transform is performed to identify the oscillatory information, which has been shown in Figure 2d. We set the time step to 5 fs and the line width to 0.00095 cm. We labeled the identified modes 300, 400 and 730 cm^{-1} with magenta squares. It shows a strong peak at frequency of 300 and 400 cm^{-1}. The frequency of 300 cm^{-1} quantitatively equals to the energy gap between two excitonic states, which manifests the evidence of electronic coherence. The peak of 390 cm^{-1} generally The frequency represented by this peak is a combination of two vibrational frequencies (730–340 cm^{-1}). The residuals in Figure 2c shows a clear evidence of two-frequency beating in the evolution time from 200 fs to 500 fs in blue solid line, which is observed when two beating modes are closed in frequencies (300 and 340 cm^{-1}). In addition, we observe a relatively weak peak at 730 cm^{-1} in Figure 2d. We further employ the wavelet analysis of coherent dynamics and the resulting data are shown in Figure 2e,f, respectively. The detailed explanation of wavelet analysis is described in the third part of the Supporting Information. The presented data of representative traces and the rest of analysis are shown in the third part of the Supporting Information. Using this analysis, we obtain the lifetimes of coherences centered at 300 and 400 cm^{-1}, which show a clear evidence of beating dynamics in (e). These coherence could persist for more than 600 fs at 77 K when the frequency of mode is close to the energy gap. In addition, we reveal that the lifetime of vibrational coherence of 730 cm^{-1} presents a relatively longer lifetime, but with a weak amplitude. Moreover, the wavelet analysis in (f) shows the lifetime of oscillatory dynamics (300 and 340 cm^{-1}) of the charge transfer state is relatively long, which indicates that the coherent dynamics could play a role of charge transfer in PSII reaction center with the strong excitonic interaction between radical pair. Furthermore, the high-frequency mode of 730 cm^{-1} shows a weak evidence of oscillation in Figure 2f.
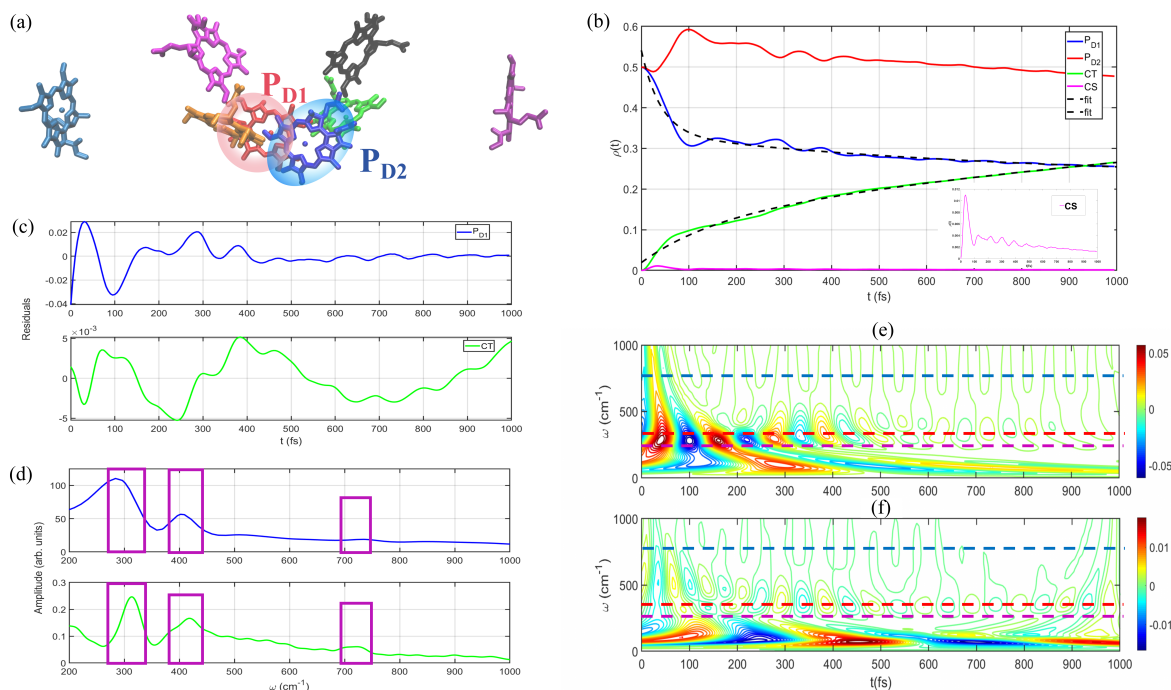

Figure 2. (a) The arrangement of pigments (P_{D1} and P_{D2}). (b) The population dynamics of the radical pair (P_{D1} and P_{D2}), charge transfer (CT) and charge separation (CS) states calculated at 77 K. Time-resolved residuals and FFT results are shown in (c,d). The peaks are marked as magenta boxes in (d). The wavelet analysis of residuals (P_{D1} and CT) are shown in (e,f), respectively.

We also examine the coherent dynamics of radial pair P_{D1} and P_{D2} at physiological temperature. For this, we changed the temperature to 300 K in the modeling and performed the calculations without any further changes. We show the calculated results in Figure 3a. The population transfers of excitonic, charge transfer and charge separations states are plotted as solid lines, respectively. We observe that the oscillatory dynamics are significantly shorten due to the increase in the temperature. Moreover, the transfer speed from exciton states to charge transfer state is dramatically increased, which has been demonstrated by exponential fitting results in Figures S1 and S2 of the second part of the Supporting Information. We perform the global fitting procedure and obtain the residuals in Figure 3b. The resulting data of Fourier transform is shown in Figure 3c, and the identified peaks are marked as square with magenta color. The peak at 730 cm^{-1} shows a weak amplitude and it manifests the vibrational coherence of high-frequency mode assigned from modeling. Interestingly, we also observe two peaks at around 300 and 360 cm^{-1} with relatively a stronger magnitude. The residuals plotted in Figure 3b indicates the beating dynamics (around 300 fs to 700 fs) between two excitonic states of P_{D1} and P_{D2}, even at room temperature, which implies that the interplay of electronic coherence 300 cm^{-1} and vibrational coherence 340 cm^{-1} could be resonantly enhanced with the strong excitonic coupling V = 150 cm^{-1}. The calculated results clearly show that the vibronic quantum coherence in radical pair could persist for a relatively long time (∼600 fs), even at room temperature. However, due to the strong dissipation, the oscillatory dynamics of charge transfer and charge separation states are missing, which can be clearly identified from the population dynamics and the associated oscillations in residuals from Figure 3a,b, respectively. We further perform the wavelet analysis and plot the results in Figure 3d,e. Based on our calculations, we only observe that the electronic coherence of charge transfer and charge separation disappear within 200 fs, which has been shown in Figure 3e.
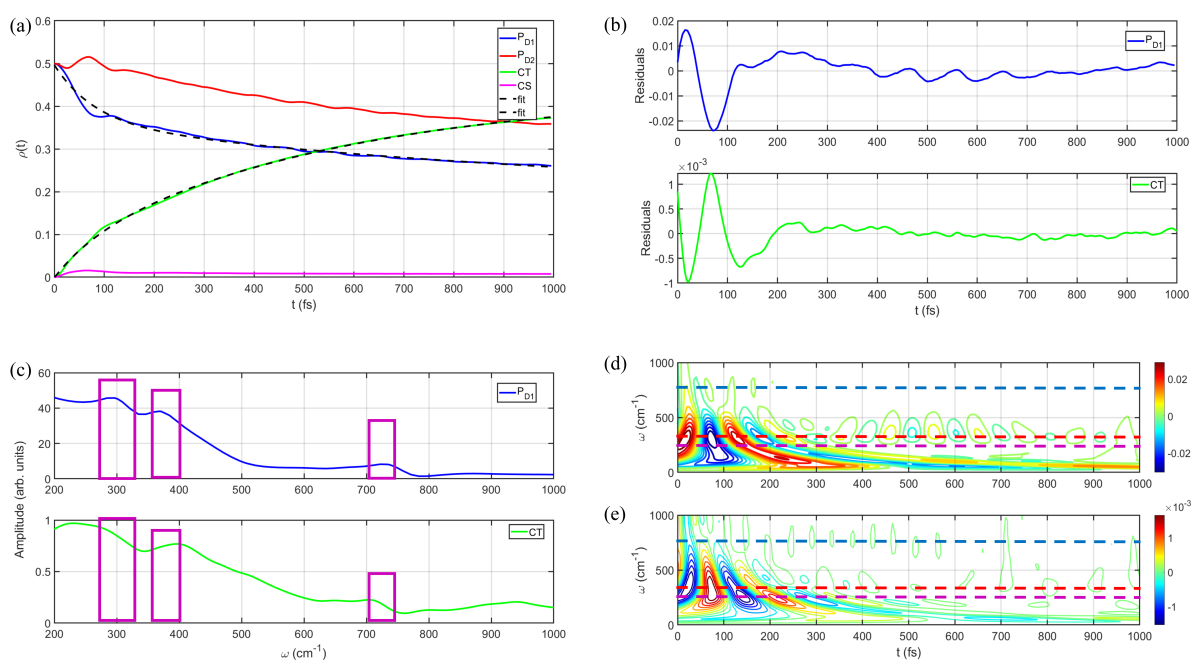

Figure 3. (**a**) Population dynamics of P_{D1}, P_{D2}, CT and CS states at 300 K. Residuals and FFT results are plotted in (**b**,**c**), respectively. (**d**,**e**) show the results of wavelet analysis of P_{D1} and CT.

3.2. Population Dynamics of Chl$_{D1}$ and Pheo$_{D1}$

Next, we investigate the population and charge transfer dynamics between Chl_{D1} and $Pheo_{D1}$. The schematic picture of chlorophylls are shown in Figure 4a. For this, we firstly assign the parameters for the modeling. The site energies of Chl_{D1} and $Pheo_{D1}$ are taken from Refs. [21,22], and the values are 20 and 50 cm^{-1}, respectively. The site energies of

charge transfer and charge separation states are 740 and 510 cm^{-1}. The excitonic interaction between two pigments, V = 46 cm^{-1}. The rest of excitonic couplings are presented in Figures S3 and S4 of the second part of the Supporting Information. We use the same parameters for the spectral densities and the system–bath interactions, except the η_3 = 3.0 and η_4 = 2.0. With these parameters, we calculate the population dynamics at 77 K, and show the results in Figure 4b. The excitonic, charge transfer and charge separation states are plotted as solid lines in Figure 4b. We also repeat the procedure to fit the kinetics and plot the residuals in Figure 4c. We observe the clear oscillatory dynamics in exctionic and charge transfer states. To examine these oscillations, we perform the Fourier transform of residuals and plot the resulting data in Figure 4d. The identified peaks are marked as squares with magenta color. We observe that, in the high-frequency region, the peak of 730 cm^{-1} with a weak amplitude manifests the vibrational coherence. The peak of 340 cm^{-1} indicates the vibrational coherence from the assigned mode in the modeling. Based on our modeling, the electronic coherence between Chl_{D1} and $Pheo_{D1}$ is at 96 cm^{-1}. We observe a broadband peak at around 96 cm^{-1} in Figure 4d, which indicates the lifetime of electronic coherence between Chl_{D1} and $Pheo_{D1}$ is short, even at low temperature. To determine the timescale precisely, we perform the wavelet analysis of residuals and plot the resulting data in Figure 4e,f, respectively. We observe, the population of excitonic state $Pheo_{D1}$, the electronic quantum coherence at around 96 cm^{-1} (magenta dashed arrow) persists for 400 fs at 77 K. The results of wavelet analysis only show a weak evidence of vibrational coherence at 730 cm^{-1} in Figure 4f.
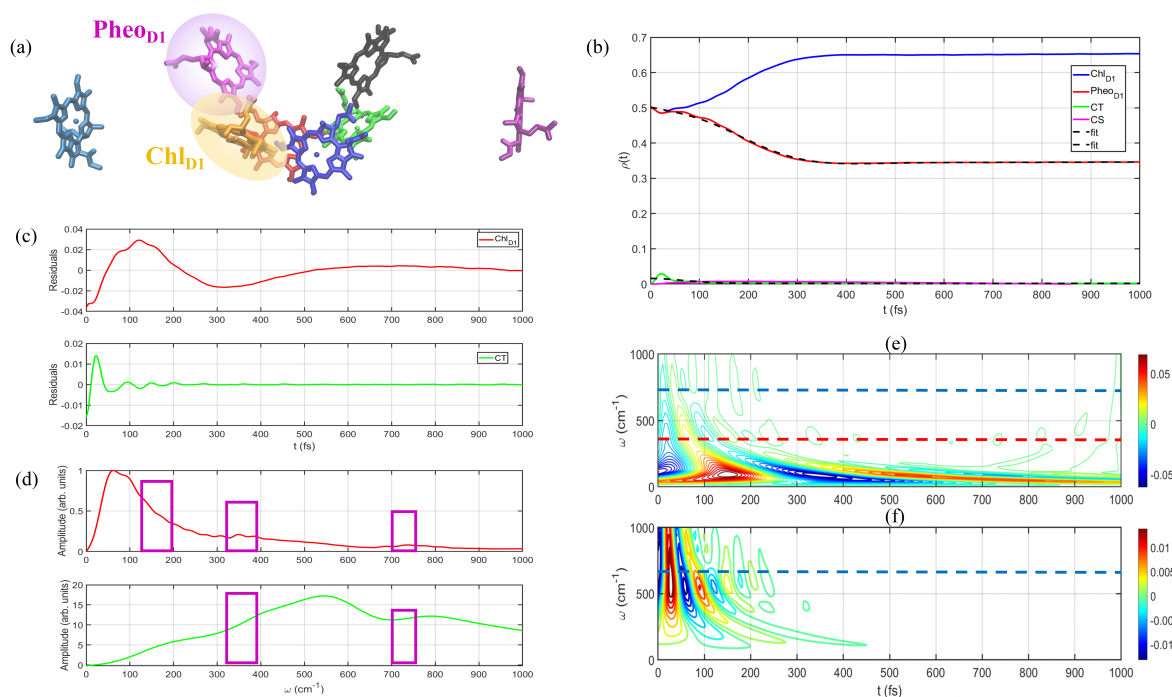

Figure 4. (**a**) Pigment arrangement of Chl_{D1} and $Pheo_{D1}$. (**b**) The population dynamics of Chl_{D1}, $Pheo_{D1}$, CT and CS states. The time-resolved residuals and FFT results are shown in (**c**,**d**), respectively. (**e**,**f**) show the results of wavelet analysis.

We further calculate the population dynamics at 300 K. The resulting data are shown in Figure 5a. The residuals and the associated Fourier transform are plotted in Figure 5b,c. We observe a clear evidence of oscillatory dynamics of residuals. Based on the Fourier transform, we identify two peaks at 340 and 730 cm^{-1}, respectively. These modes reveal the vibrational coherence presented in the oscillations of residuals. Moreover, the vibrational coherence of 340 cm^{-1} could be clearly observed in charge transfer state. In addition, the associated wavelet analyses are presented in Figure 5d. However, we do not observe

any evidence of electronic coherence of excitonic states of Chl_{D1} and $Pheo_{D1}$. Thus, we conclude that, in the second pathway of charge transfer, the electronic coherence could not persist for a long time, even at low temperature, due to the relatively weak magnitude of excitonic interaction, V = 46 cm^{-1}.
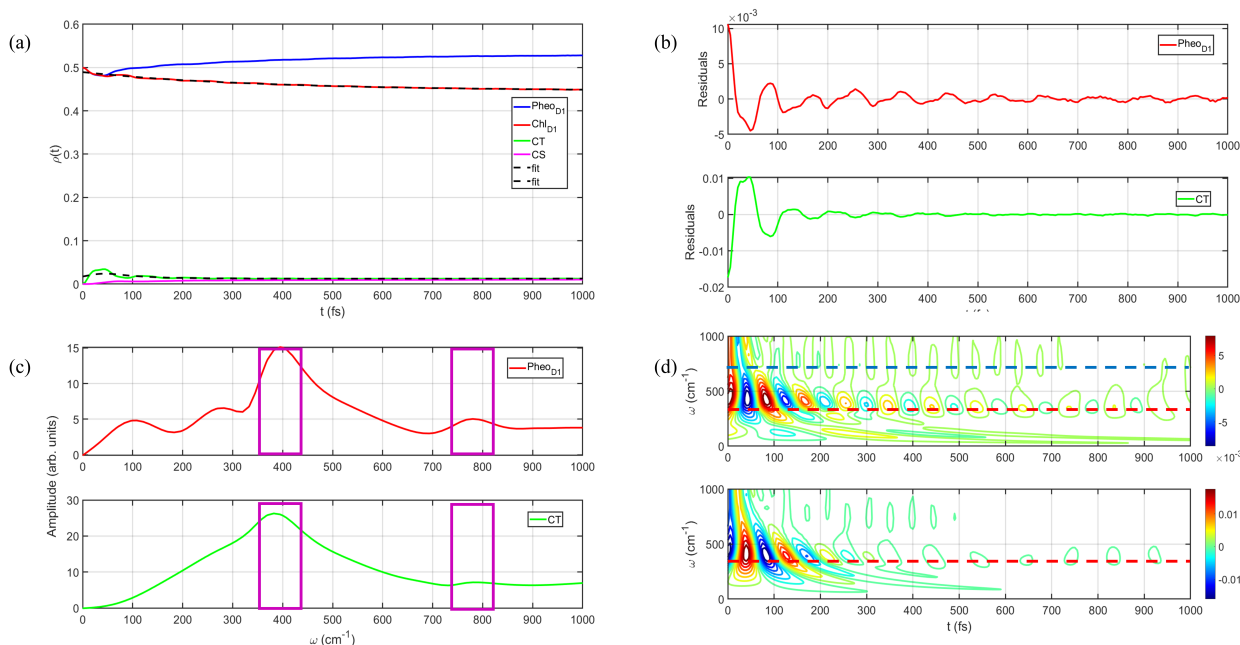

Figure 5. (**a**) The population dynamics of Chl_{D1}, $Pheo_{D1}$, CT and CS states. The residuals and FFT results are shown in (**b**,**c**), respectively. The wavelet analysis of Chl_{D1} and CT are plotted in (**d**).

4. Discussions

Based on the above calculations, we could conclude that the lifetime of electronic quantum coherence between Chl_{D1} and $Pheo_{D1}$ is quite short. The spatial distance of two pigments is longer than 3 $\mathring{A}$, which results in a value of 46 cm^{-1} for excitonic coupling. This value indicates that the interaction between Chl_{D1} and $Pheo_{D1}$ is in the intermediate region of photosynthetic protein complexes, which is comparable to the value of other photosynthetic complexes responsible for energy transfer; for instance, the Fenna–Matthews–Olson complex and light-harvesting complex II. Thus, we safely conclude that the electronic coherence between pigments within the weak or intermediate region of couplings do not persist for a long time, even at lower temperatures. Moreover, we observe that the long-lived vibrational coherence in the charge transfer and charge separation states, even with strong dissipation of these states from protein environment. Due to the short lifetime of electronic coherence, the long-lived vibrational coherences can not enhance the electronic coherence to construct the vibronic coherence, even in the resonant case [25].

However, it shows a completely different picture of coherent dynamics in the radical pair. Based on its protein structure, the distance between P_{D1} and P_{D2} is less than 3 $\mathring{A}$, which results in a strong overlap between two pigments, which naturally induce a charge transfer state with a strong excitonic coupling V = 150 cm^{-1}. This value of excitonic coupling is much stronger than the averaged value in photosynthetic protein complexes, and is only present in the reaction center. It is a unique structure in the natural photosynthetic protein complex. Based on our modeling, we demonstrated that the electronic coherence between P_{D1} and P_{D2} could persist for a long time, and the interplay between electronic coherence and vibrational coherence prolong the lifetime of vibronic coherence. Moreover, this observed coherence could survive for a relatively long time even at room temperature. We believe this strong excitonic coupling results in the long-lived coherence, which could enhance the speed and efficiency of charge transfer and charge separation in PSII reaction center.

It has been calculated that a strong transition dipole and short distance in molecular crystals results in strong excitonic couplings between molecules; for instance, the molecular crystals of pentacene and tetracene [26]. The recent studies of population transfers and the dynamics from singlet to triplet states in singlet fission have been intensively studied by ultrafast spectroscopy [27,28]. More recently, Ralph et al. studied the dynamics of singlet fission by transient ARPES, and revealed the process is fully mediated by electronic charge-states states [29]. Based on this study, we predict that the strong excitonic couplings between molecules could induce a relatively long timescale of electronic coherence in the molecular crystals. However, we also uncovered that the interplay of Holstein and Peierls modes could effectively destroy the electronic coherence by opening a new deactivation channel between two potential energy surfaces [30,31].

5. Conclusions

In this paper, we studied the photo-induced energy and charge transfer dynamics in two pathways of the PSII reaction center. To examine the underlying coherent dynamics during these processes, we selected a two dimer model with charge transfer and charge separation states. Additionally, two vibrational modes were selected, and included in the dimer system to study the interplay between the electronic and vibrational coherences. Based on our calculations, we observed that, due to the strong excitonic interaction, the radical pair (P_{D1} and P_{D2}) shows a long-lived electronic coherence. Furthermore, we observed that, in the strong coupling region, the vibronic coupling could prolong the oscillatory dynamics in the resonant case. Interestingly, this observed coherence could survive for a relatively long lifetime, even at room temperature. We imply that this coherence could be critical for the charge transfer and charge separation dynamics in the PSII reaction center. However, with a relatively weaker excitonic coupling, the second pathway of charge transfer between Chl_{D1} and $Pheo_{D1}$ does not present any evidence of long-lived electronic coherence, even at 77 K. In addition, we demonstrated that, due to the short lifetime, the electronic coherence can not be enhanced by vibrational coherence, even in the resonance case. Based on these results, we conclude that the electronic quantum coherence could play a role in charge transfer dynamics in PSII reaction center, but only in the case of strong excitonic coupling in radical pair. The electronic coherence may barely be enhanced in the intermediate region of excitonic coupling. Thus, we envision that the uncovered physical insight gained form our work can be used for the rational design of energy and charge transfers in the artificial light harvesting systems.

Author Contributions: H.-G.D., P.-P.Z. conceived the research and discussed with A.J., V.T., P.-P.Z., J.Z., X.Z. and H.-G.D. performed the theoretical calculations. H.-G.D., P.-P.Z and A.J. wrote the first draft and refined by all authors. H.-G.D. supervised this project. Software, C.M. All authors have read and agreed to the published version of the manuscript.

Institutional Review Board Statement: Not Applicable.

Informed Consent Statement: Not Applicable.

Data Availability Statement: The data that support the findings of this study are available from the corresponding author upon reasonable request.

References

1. Umena, Y.; Kawakami, K.; Shen, J.R.; Kamiya, N. Crystal structure of oxygen-evolving Photosystem II at a resolution of 1.9A. *Nature* **2011**, *473*, 55–60. [CrossRef] [PubMed]
2. Dods, R.; Båth, P.; Morozov, D.; Gagnér, V.A.; Arnlund, D.; Luk, H.L.; Kübel, J.; Maj, M.; Vallejos, A.; Wickstrand, C.; et al. Ultrafast structural changes within a photosynthetic reaction center. *Nature* **2020**, *589*, 310–314. [CrossRef]
3. Suga, M.; Akita, F.; Hirata, K.; Ueno, G.; Murakami, H.; Nakajima, Y.; Shimizu, T.; Yamashita, K.; Yamamoto, M.; Ago, H.; et al. Native structure of photosystem II at 1.95 resolution viewed by femtosecond X-ray pulses. *Nature* **2015**, *517*, 99. [CrossRef]
4. Diner, B.A.; Rappaport, F. Structure, dynamics, and energetics of the primary photochemistry of Photosystem II of oxygenic photosynthesis. *Annu. Rev. Plant Biol.* **2002**, *53*, 551–580. [CrossRef]
5. Lewis, K.L.M.; Fuller, F.D.; Myers, J.A.; Yocum, C.F.; Mukamel, S.; Abramavicius, D.; Ogilvie, J. Simulation of the two-dimensional electronic spectroscopy of the photosystem II reaction center. *J. Phys. Chem. A* **2013**, *117*, 34–41. [CrossRef]
6. Novoderezhkin, V.I.; Andrizhiyevskaya, E.G.; Dekker, J.P.; van Grondelle, R. Pathways and Timescales of Primary Charge Separation in the Photosystem II Reaction Center as Revealed by a Simultaneous Fit of Time-Resolved Fluorescence and Transient Absorption. *Biophys. J.* **2005**, *89*, 1464–1481. [CrossRef]
7. Yoneda, Y.; Arsenault, E.A.; Yang, S.-J.; Orcutt, K.; Iwai, M.; Fleming, G.R. The initial charge separation step in oxygenic photosynthesis. *Nat. Commun.* **2022**, *13*, 2275. [CrossRef]
8. Prokhorenko, V.I.; Holzwarth, A.R. Primary processes and structure of the Photosystem II reaction center: A photon echo study. *J. Phys. Chem. B* **2000**, *104*, 11563–11578. [CrossRef]
9. Romero, E.; Van Stokkum, I.H.; Novoderezhkin, V.I.; Dekker, J.P.; Van Grondelle, R. Two different charge separation pathways in Photosystem, I.I. *Biochemistry* **2010**, *49*, 4300–4307. [CrossRef]
10. Duan, H.G.; Prokhorenko, V.I.; Cogdell, R.J.; Ashraf, K.; Stevens, A.L.; Thorwart, M.; Miller, R.J.D. Nature does not rely on long-lived electronic quantum coherence for photosynthetic energy transfer. *Proc. Natl. Acad. Sci. USA* **2017**, *114*, 8493–8498. [CrossRef]
11. Scholes, G.D.; Fleming, G.R.; Chen, L.X.; Aspuru-Guzik, A.; Buchleitner, A.; Coker, D.F.; Engel, G.; Van Grondelle, R.; Ishizaki, A.; Jonas, D.; et al. Using coherence to enhance function in chemical and biophysical systems. *Nature* **2017**, *543*, 647–656. [CrossRef] [PubMed]
12. Thyrhaug, E.; Tempelaar, R.; Alcocer, M.J.P.; Žídek, K.; Bína, D.; Knoester, J.; Jansen, T.L.C.; Zigmantas, D. Identification and characterization of diverse coherences in the Fenna–Matthews–Olson complex. *Nat. Chem.* **2018**, *10*, 780–786. [CrossRef] [PubMed]
13. Duan, H.G.; Jha, A.; Chen, L.; Tiwari, V.; Cogdell, R.J.; Ashraf, K.; Prokhorenko, V.I.; Thorwart, M.; Miller, R.D. Quantum coherent energy transport in the Fenna–Matthews–Olson complex at low temperature. *Proc. Natl. Acad. Sci. USA* **2022**, *119*, e2212630119. [CrossRef] [PubMed]
14. Wang, L.; Allodi, M.A.; Engel, G.S. Quantum coherences reveal excited-state dynamics in biophysical systems. *Nat. Rev. Chem.* **2019**, *3*, 477–490. [CrossRef]
15. Romero, E.; Novoderezhkin, V.I.; Grondelle van, R. Quantum design of photosynthesis for bio-inspired solar-energy conversion. *Nature* **2017**, *543*, 355–365. [CrossRef] [PubMed]
16. Myers, J.A.; Lewis, K.L.; Fuller, F.D.; Tekavec, P.F.; Yocum, C.F.; Ogilvie, J.P. Two-dimensional electronic spectroscopy of the D1-D2-cyt b559 photosystem II reaction centre complex. *J. Phys. Chem. Lett.* **2010**, *1*, 2774–2780. [CrossRef]
17. Fuller, F.D.; Pan, J.; Gelzinis, A.; Butkus, V.; Senlik, S.S.; Wilcox, D.E.; Yocum, C.F.; Valkunas, L.; Abramavicius, D.; Ogilvie, J.P. Vibronic coherence in oxygenic photosynthesis. *Nat. Chem.* **2014**, *6*, 706–711. [CrossRef]
18. Romero, E.; Augulis, R.; Novoderezhkin, V.I.; Ferretti, M.; Thieme, J.; Zigmantas, D.; Van Grondelle, R. Quantum coherence in photosynthesis for efficient solar-energy conversion. *Nat. Phys.* **2014**, *10*, 676–682. [CrossRef]
19. Novoderezhkin, V.I.; Dekker, J.P.; van Grondelle, R. Mixing of Exciton and Charge-transfer states in Photosystem II Reaction centers: Modeling of Stark Spectra with Modified Redfield Theory. *Biophys. J.* **2007**, *93*, 1293–1311. [CrossRef]
20. Novoderezhkin, V.I.; Romero, E.; Dekker, J.P.; van Grondelle, R. Multiple Charge-separation pathways in photosystem II: Modeling of transient absorption kinetics. *Chem. Phys. Chem.* **2011**, *12*, 681–688. [CrossRef]
21. Gelzinis, A.; Valkunas, L.; Fuller, F.D.; Ogilvie, J.P.; Mukamel, S.; Abramavicius, D. Tight-binding model of the photosystem II reaction center: Application to two-dimensional electronic spectroscopy. *New J. Phys.* **2013**, *15*, 075013. [CrossRef]
22. Jha, A.; Zhang, P.-P.; Tiwari, V.; Chen, L.; Thorwart, M.; Miller, R.J.D.; Duan, H.-G. Unraveling Quantum Coherences Mediating Primary Charge Transfer Processes in Photosystem II Reaction Center. Science Advances, accepted for publication. *Sci. Adv.* **2024**, *10*, eadk1312. [CrossRef] [PubMed]
23. Song, Y.; Sechrist, R.; Nguyen, H.H.; Johnson, W.; Abramavicius, D.; Redding, K.E.; Ogilvie, J.P. Excitonic structure and charge separation in the heliobacterial reaction center probed by multispectral multidimensional spectroscopy. *Nat. Commun.* **2021**, *12*, 2801. [CrossRef] [PubMed]
24. Prokhorenko, V.I. Global analysis of multi-dimensional experimental data. *Eur. Photochem. Assoc. Newslett.* **2012**, 21–23.
25. Duan, H.G.; Thorwart, M.; Miller, R.J. Does electronic coherence enhance anticorrelated pigment vibrations under realistic conditions? *J. Chem. Phys.* **2019**, *151*, 114115. [CrossRef] [PubMed]
26. Girl, A.; Grisanti, L.; Masino, M.; Brillante, A.; Della Valle, R.G.; Venuti, E. Interaction of charge carriers with lattice and molecular phonons in crystalline pentacene. *J. Chem. Phys.* **2011**, *135*, 084701.

27. Bakulin, A.A.; Morgan, S.E.; Kehoe, T.B.; Wilson, M.W.B.; Chin, A.W.; Zigmantas, D.; Egorova, D.; Rao, A. Real-time observation of multiexcitonic states in ultrafast singlet fission using coherent 2D electronic spectroscopy. *Nat. Chem.* **2016**, *8*, 16. [CrossRef] [PubMed]

28. Miyata, K.; Kurashige, Y.; Watanabe, K.; Sugimoto, T.; Takahashi, S.; Tanaka, S.; Takeya, J.; Yanai, T.; Matsumoto, Y. Coherent singlet fission activated by symmetry breaking. *Nature Chem.* **2017**, *9*, 983. [CrossRef] [PubMed]

29. Neef, A.; Beaulieu, S.; Hammer, S.; Dong, S.; Maklar, J.; Pincelli, T.; Xian, R.P.; Wolf, M.; Rettig, L.; Pflaum, J.; et al. Orbital-resolved observation of singlet fission. *Nature* **2023**, *616*, 275. [CrossRef]

30. Duan, H.G.; Nalbach, P.; Miller, R.D.; Thorwart, M. Ultrafast Energy Transfer in Excitonically Coupled Molecules Induced by a Nonlocal Peierls Phonon. *J. Phys. Chem. Lett.* **2019**, *10*, 1206. [CrossRef]

31. Duan, H.G.; Jha, A.; Li, X.; Tiwari, V.; Ye, H.; Nayak, P.K.; Zhu, X.L.; Li, Z.; Martinez, T.J.; Thorwart, M.; et al. Intermolecular vibrations mediate ultrafast singlet fission. *Sci. Adv.* **2020**, *6*, eabb0052. [CrossRef] [PubMed]